Journal of Organometallic Chemistry 693 (2008) 2327–2337

Contents lists available at ScienceDirect

Journal of Organometallic Chemistry

journal homepage: www.elsevier.com/locate/jorganchem

CO substitution in $HRu_3(CO)_{10}(\mu$-COMe) by the unsaturated diphosphine ligand 4,5-bis(diphenylphosphino)-4-cyclopenten-1,3-dione (bpcd): Synthesis and reactivity studies of the face-capped cluster $Ru_3(CO)_7(\mu_3$-COMe)[μ-P(Ph)C=C(PPh_2)C(O)CH_2C(O)]

Simon G. Bott [a,*], Huafeng Shen [b], Shih-Huang Huang [b], Michael G. Richmond [b,*]

[a] Department of Chemistry, University of Houston, Houston, TX 77004, United States
[b] Department of Chemistry, University of North Texas, Denton, TX 76203, United States

ARTICLE INFO

Article history:
Received 15 March 2008
Received in revised form 2 April 2008
Accepted 2 April 2008
Available online 10 April 2008

Keywords:
Ruthenium clusters
Ligand substitution
Diphosphine ligand
P–C bond activation
Cluster expansion

ABSTRACT

The reaction of the methylidyne-bridged cluster $HRu_3(CO)_{10}(\mu$-COMe) (**1**) with the diphosphine ligand 4,5-bis(diphenylphosphino)-4-cyclopenten-1,3-dione (bpcd) and Me_3NO furnishes $HRu_3(CO)_8(\mu$-COMe)(bpcd) (**2**) and $HRu_3(CO)_8(Ph_2PH)[\mu$-PPh_2C=CC(O)CH_2C(O)] (**3**) as the major and minor products, respectively. The ^{1}H and ^{31}P NMR data indicate that the bpcd ligand in **2** is chelated to one of the ruthenium atoms that is bridged by the hydride and methylidyne ligands. Thermolysis of **2** is accompanied by P–Ph bond cleavage and elimination of benzene to yield $Ru_3(CO)_7(\mu_3$-COMe)[μ-P(Ph)C=C(PPh_2)C(O)CH_2C(O)] (**4**). Compound **4** consists of a triangular ruthenium core that is face-capped by μ_3-COMe methylidyne and μ-P(Ph)C=C(PPh_2)C(O)CH_2C(O) phosphido ligands. The kinetics for the conversion of **2** → **4** have been measured in toluene solvent over the temperature range 320–343 K, and based on the observed activation parameters and the inhibitory effect of added CO on the reaction, a rate-limiting step involving a dissociative loss of CO is supported. Heating **4** in the presence of H_2 afforded the phosphinidene-capped cluster $H_3Ru_3(CO)_7(\mu_3$-PPh)[μ-C=C(PPh_2)C(O)CH_2C(O)] (**5**). Crystallographic analysis of **5** has confirmed the loss of the methylidyne moiety and the cleavage of the phosphido PhP–C(dione) bond, and the presence of three edge-bridging hydrides is supported by ^{1}H NMR spectroscopy. The reaction of **4** with added PPh_3 and PMe_3 has been investigated; the uptake of a single phosphine ligand occurs regiospecifically at one of the phosphido-bound ruthenium centers to give $Ru_3(CO)_6L(\mu_3$-COMe)[μ-P(Ph)C=C(PPh_2)C(O)CH_2C(O)] (PPh_3, **6**; PMe_3, **7**). Compound **6** contains 48e- and exhibits a structural motif similar to that found in **4**. Compound **7** readily adds a second PMe_3 ligand to yield the bis-substituted cluster $Ru_3(CO)_6(PMe_3)_2(\mu_2$-COMe)[$\mu$-P(Ph)C=C($PPh_2$)C(O)$CH_2$C(O)] (**8**). The solid-state structure of **8** confirms the loss of two ruthenium–ruthenium bonds and the conversion of the original face-capping μ_3-COMe ligand to a μ_2-COMe moiety that tethers two non-bonding ruthenium centers. The two PMe_3 ligands in **8** coordinate to the same ruthenium center, and the 9e- P(Ph)C=C(PPh_2)C(O)CH_2C(O) ligand binds all three ruthenium atoms through the phosphine, phosphido, alkene, and carbonyl moieties. Near-UV irradiation of **8** leads to loss of CO and polyhedral contraction of the triruthenium frame to yield the 48e- cluster $Ru_3(CO)_5(PMe_3)_2(\mu_3$-COMe)[$\mu$-P(Ph)C=C($PPh_2$)C(O)$CH_2$C(O)] (**9**).

1. Introduction

Activation of the methylidyne-bridged cluster $HRu_3(CO)_{10}(\mu$-COMe) (**1**) by the oxidative-decarbonylation reagent Me_3NO in the presence of the rigid diphosphine ligand 2,3-bis(diphenylphosphino)maleic anhydride (bma) gives the chelated cluster $HRu_3(CO)_8$(bma)(μ-COMe) and the diphenylphosphine-substituted cluster $HRu_3(CO)_8(Ph_2PH)[\mu$-PPh_2C=CC(O)OC(O)] as the major and minor products, respectively [1]. Eq. (1) summarizes the reaction between **1** and the bma ligand. Controlled thermolysis of **1** with bma yields only trace amounts of $HRu_3(CO)_8$(bma)(μ-COMe) due to its facile decomposition under the reaction conditions. Also exacerbating the situation is the extensive loss of all bma-substituted products during chromatographic work-up due to the deleterious support-induced hydrolysis of the anhydride ring [2].

* Corresponding authors. Tel.: +1 713 743 2771 (S.G. Bott); tel.: +1 940 565 3548 (M.G. Richmond).
E-mail addresses: sbott@uh.edu (S.G. Bott), cobalt@unt.edu (M.G. Richmond).

0022-328X/$ - see front matter © 2008 Elsevier B.V. All rights reserved.
doi:10.1016/j.jorganchem.2008.04.007

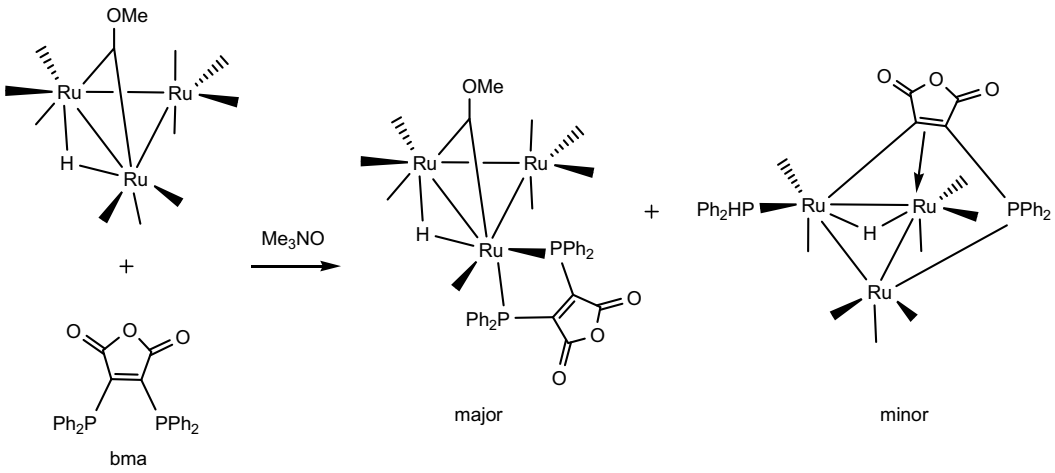

(1)

Since a detailed mechanistic study on the degradation pathway(s) exhibited by the bma-chelated cluster $HRu_3(CO)_8(bma)(\mu\text{-}COMe)$ during thermolysis and was hampered, in part, due to the unavoidable decomposition of the bma-derived products during chromatographic separation, the reaction between **1** and the related diphosphine ligand 4,5-bis(diphenylphosphino)-4-cyclopenten-1,3-dione (bpcd) was next explored. While both ligands are structurally similar in terms of the their cluster binding properties, the dione moiety associated with the bpcd ligand is stable to chromatographic supports. Treatment of **1** with bpcd in the presence of Me_3NO furnishes the bpcd-chelated cluster $HRu_3(CO)_8(bpcd)(\mu\text{-}COMe)$ (**2**), which unlike its bma counterpart $HRu_3(CO)_8(bma)(\mu\text{-}COMe)$, is easily purified by column chromatography and isolated in high yields. The ready availability of **2** has greatly facilitated our investigation on the reactivity of the ancillary methylidyne and bpcd ligands in this and other related clusters under thermal and photochemical activation. Previous reports from our groups have demonstrated low-energy manifolds for the activation of the diphosphine ligands bma and bpcd in a variety of polynuclear systems containing face-capping carbyne and alkyne ligands [3].

2. Experimental

2.1. General

The carbonylation of $RuCl_3 \cdot xH_2O$ to give $Ru_3(CO)_{12}$ was conducted in a 1000 mL Parr Series 4000 rocking autoclave and employed the procedure of Bruce [4], while the starting cluster **1** was prepared according to the procedure of Keister et al. [5]. The bpcd ligand used in this study was synthesized from 4,5-dichloro-4-cyclopenten-1,3-dione and Ph_2PSiMe_3 [6]. All reaction solvents were distilled from an appropriate drying agent under argon using Schlenk techniques and stored in Schlenk storage vessels equipped with high-vacuum Teflon stopcocks [7]. The IR and NMR solvents were reagent grade and were typically degassed by three pump-thaw-degas cycles prior to their use. The reported combustion analyses were performed by Atlantic Microlab, Norcross, GA.

The infrared spectra were recorded on a Nicolet 20 SXB FT-IR spectrometer in a 0.1 mm NaCl cell, using PC control and OMNIC software. The reported ^1H and ^{31}P NMR spectra were recorded at 200 MHz on a Varian Gemini-200 spectrometer and 121 MHz on a Varian 300-VXR spectrometer, respectively. The reported ^{31}P chemical shifts, which were recorded in the proton-decoupled mode unless otherwise stated, are referenced to external H_3PO_4 (85%), taken to have $\delta = 0$. The reported ESI mass spectral data for cluster **9** were collected at the UNT mass spectrometry facility in the positive ion mode, using a MeOH matrix containing 1% AcOH. The spectroscopic data for clusters **2**–**9** are summarized in Table 1.

2.2. Reaction of $HRu_3(CO)_{10}(\mu\text{-}COMe)$ with bpcd in the presence of Me_3NO to give $HRu_3(CO)_8(\mu\text{-}COMe)(bpcd)$ (**2**) and $HRu_3(CO)_8(Ph_2PH)[\mu\text{-}PPh_2C{=}CC(O)CH_2C(O)]$ (**3**)

To 0.35 g (0.52 mmol) of **1** and 0.27 g (0.58 mmol) of bpcd in a large Schlenk flask under argon was added 50 mL of CH_2Cl_2 by cannula. The solution was stirred at room temperature for 1 h and then examined by both TLC and IR spectroscopy. Only the two reactants were observed, at which point 84 mg (1.1 mmol) of Me_3NO was next added, causing an immediate change in the color of the solution from red to yellow-brown. Stirring was continued for an additional 0.5 h and the solution was examined by TLC, which revealed the presence of one major yellow-brown spot corresponding to **2** ($R_f = 0.25$ using 1:1 CH_2Cl_2/hexane), in addition to a trace amount of **1** ($R_f = 0.90$ same eluent) and red-black material at the origin of the plate. After the solvent was removed under vacuum, the residue was purified by column chromatography over silica using hexane to first elute unreacted **1**, after which the mobile phase was changed to CH_2Cl_2 to furnish **2**. Washing the column with acetone allowed for the separation of a small amount of the red **3**. Both new products were recrystallized from benzene/hexane at room temperature to yield 0.46 g (82%) of **2** and 15 mg (2.9%) of **3**. Compound **2**: Anal. Calc. for $C_{39}H_{26}O_{11}P_2Ru_3 \cdot 1/4C_6H_6$: C, 46.05; H, 2.61. Found: C, 45.89; H, 2.85%. Compound **3**: Anal. Calc. for $C_{37}H_{24}O_{10}P_2Ru_3 \cdot 1/2C_6H_6$: C, 46.48; H, 2.61. Found: C, 46.34; H, 2.69%.

2.3. Thermolysis of $HRu_3(CO)_8(\mu_2\text{-}COMe)(bpcd)$ (**2**) to $Ru_3(CO)_7(\mu_3\text{-}COMe)[\mu\text{-}P(Ph)C{=}C(PPh_2)C(O)CH_2C(O)]$ (**4**)

To a Schlenk tube was charged 0.20 g (0.19 mmol) of **2** under argon flush, followed by 30 mL of 1,2-dichloroethane (DCE). The vessel was sealed and heated at ca. 80–90 °C for period of 2 h, with the solution slowly turning from yellow-brown to red in color. Upon cooling, TLC analysis using a 10:1 mixture of CH_2Cl_2/acetone as the eluent revealed trace amounts of **1** ($R_f = 0.95$) and **2** ($R_f = 0.60$), along with a large red spot corresponding to **4** ($R_f = 0.25$) and some black material at the origin. The solvent was removed and **4** subsequently isolated by column chromatography using the aforementioned eluent. The desired product was recrys-

Table 1
IR and NMR spectroscopic data for the triruthenium clusters **2–9**

Cluster	IR[a] (cm^{-1})	^{31}P NMR, δ[b]	^{1}H NMR, δ
2	2074 (s), 2037 (vs), 2000 (s), 1982 (s), 1974 (s), 1946 (w, sh), 1746 (w, sym dione), 1714 (m, antisym dione)	51.74 (s), 43.62 (s)	7.00–8.20 (m, 20H, aryl), 4.07 (s, 3H, OMe), 3.41 (AB quartet, 2H, CH_2, $^2J_{H-H}$ = 22 Hz), −13.29 (t, 1H, hydride, $^2J_{P-H}$ = 7 Hz)
3	2079 (s), 2039 (vs), 2027 (vs), 1980 (s), 1712 (m, sym dione), 1682 (m, antisym dione)	32.28 [s, Ph_2P(dione)], 7.70 (s, Ph_2PH)	6.83–7.80 (m, 20H, aryl), 6.89 (d, 1H, Ph_2PH, $^1J_{P-H}$ = 388 Hz), 3.01 (AB quartet, 2H, CH_2, $^2J_{H-H}$ = 22 Hz), −13.34 (dd, 1H, hydride, $^2J_{P-H}$ = 12, 18 Hz)
4	2075 (s), 2020 (vs), 1978 (m), 1968 (m), 1708 (m, sym dione), 1684 (m, antisym dione)	83.15 (d, μ_2-phosphido, $^2J_{P-P}$ = 9 Hz), 37.15 (d, phosphine, $^2J_{P-P}$ = 9 Hz)	7.20–7.84 (m,15H, aryl), 4.54 (s, 3H, OMe), 3.51 (AB quartet, 2H, CH_2, $^2J_{H-H}$ = 22 Hz)
5	2101 (s), 2041 (vs), 1933 (s), 1722 (w, sym dione), 1689 (m, antisym dione)	259.32 (s, μ_3-phosphido), 18.17 (s, phosphine)	7.05–7.80 (m, 15H, aryl), 2.95 (s, 2H, CH_2), −17.41 (br t, 1H, hydride, J = 15 Hz), −18.25 (br d, 1H, hydride, J = 15 Hz), −18.70 (br m, 1H, hydride)
6	2027 (m), 2000 (vs), 1966 (s), 1707 (m, sym dione), 1681 (m, antisym dione)	85.01 (dd, μ_2-phosphido, J_{P-P} = 156, 7 Hz), 42.21 (d, PPh_3, J_{P-P} = 156 Hz), 41.08 (d, phosphine, J_{P-P} = 7 Hz)	7.10–7.90 (m, 30H, aryl), 3.45 (AB quartet, 2H, CH_2, $^2J_{H-H}$ = 21 Hz), 3.02 (s, 3H, OMe)
7	2032 (m), 2002 (vs), 1968 (m), 1944 (sh), 1693 (m, sym dione), 1670 (m, antisym dione)	80.95 (dd, μ_2-phosphido, J_{P-P} = 19, 15 Hz), 39.22 (dd, phosphine, J_{P-P} = 32, 15 Hz), −10.40 (dd, PMe_3, J_{P-P} = 32, 19 Hz)	7.05–7.95(m, 15H, aryl), 4.56 (s, 3H, OMe), 3.53 (AB quartet, 2H, CH_2, $^2J_{H-H}$ = 21 Hz), 1.64 (d, 9H, PMe_3, $^2J_{P-H}$ = 10 Hz)
8	2051 (vs), 1994 (s), 1975 (s), 1942 (m), 1906 (m), 1637 (m, free dione CO)	27.93 (d, phosphine, J_{P-P} = 22 Hz), 2.12 (dd, PMe_3, J_{P-P} = 244, 22 Hz), −12.27 (t, PMe_3, J_{P-P} = 22 Hz), −52.15 (dt, μ_2-phosphido, J_{P-P} = 244, 22 Hz)	6.48–7.70 (m, 15H, aryl), 4.42 (s, 3H, OMe), 4.20 (AB quartet, 2H, CH_2, $^2J_{H-H}$ = 21 Hz), 1.31 (d, 9H, PMe_3, $^2J_{P-H}$ = 10 Hz), 0.84 (d, 9H, PMe_3, $^2J_{P-H}$ = 10 Hz)
9	2065 (w), 2010 (vs), 1984 (vs), 1951 (vs), 1908 (s), 1675 (m, sym dione), 1650 (m, antisym dione)	73.72 (m, μ_2-phosphido), 48.50 (m, phosphine), 7.80 (m, PMe_3), −9.45 (t, PMe_3, J = 33 Hz)	6.94–7.84 (m, 15H, aryl), 4.50 (s, 3H, OMe), 3.50 (AB quartet, 2H, CH_2, $^2J_{H-H}$ = 21 Hz), 1.53 (d, 9H, PMe_3, $^2J_{P-H}$ = 10 Hz), 1.18 (d, 9H, PMe_3, $^2J_{P-H}$ = 10 Hz)

[a] All IR spectra were recorded in CH_2Cl_2.
[b] All NMR data were recorded in $CDCl_3$ at room temperature.

tallized from CH_2Cl_2/hexane to afford 0.15 g (84% yield) of **4**. Anal. Calc. for $C_{32}H_{20}O_{10}P_2Ru_3$: C, 41.34; H, 2.17. Found: C, 41.16; H, 2.12%.

2.4. Synthesis of $H_3Ru_3(CO)_7(\mu_3\text{-}PPh)[\mu\text{-}C{=}C(PPh_2)C(O)CH_2C(O)]$ (**5**) from the thermolysis of $Ru_3(CO)_7(\mu_3\text{-}COMe)[\mu\text{-}P(Ph)C{=}C(PPh_2)C(O)CH_2C(O)]$ (**4**) in the presence of hydrogen

To a Fisher-Porter tube was added 0.12 g (0.13 mmol) of **2** and 50 mL of toluene, after which the vessel was sealed and degassed via three pressurization cycles using nitrogen. The vessel was next charged with 100 psi of H_2 and stirred at room temperature for several hours and examined by TLC, which confirmed the presence of only starting cluster. The solution was then heated at ca. 60–70 °C overnight in a thermostated oil bath. Upon cooling, the solution was again examined by TLC using CH_2Cl_2 as the eluent, revealing the complete consumption of **2** and the presence of a yellow spot (R_f = 0.45) corresponding to **5**. Chromatographic separation, followed by recrystallization from CH_2Cl_2/MeOH at 0 °C, furnished 60 mg (52% yield) of **5**. Anal. Calc. for $C_{30}H_{20}O_9P_2Ru_3$: C, 40.45; H, 2.25. Found: C, 40.53; H, 2.32%.

2.5. Synthesis of $Ru_3(CO)_6(PPh_3)(\mu_3\text{-}COMe)[\mu\text{-}P(Ph)C{=}C(PPh_2)C(O)CH_2C(O)]$ (**6**) from the reaction of $Ru_3(CO)_7(\mu_3\text{-}COMe)[\mu\text{-}P(Ph)C{=}C(PPh_2)C(O)CH_2C(O)]$ (**4**) with PPh_3

The substitution reaction was carried out in medium-sized Schlenk tube under argon using 0.10 g (0.11 mmol) of **4** and 30 mg (0.11 mmol) of PPh_3 in 40 mL of CH_2Cl_2. The reactants were refluxed for ca. 2 h at room temperature and the extent of the reaction checked by TLC analysis. Other than some unreacted **4** and a trace amount of PPh_3, the presence of a red-brown spot corresponding to **6** was observed at R_f = 0.40 using 1:1 CH_2Cl_2/petroleum ether as the mobile phase. Compound **6** was isolated by column chromatography by first eluting with hexane to remove unreacted starting materials and then an eluent composed of a 10:1 mixture of CH_2Cl_2/Et_2O. Recrystallization of **6** from CH_2Cl_2 and MeOH afforded the analytical sample and single crystals suitable for X-ray diffraction analysis. Yield of **6**: 72% (90 mg). Anal. Calc. for $C_{39}H_{35}O_9P_3Ru_3 \cdot CH_2Cl_2 \cdot MeOH$: C, 47.82; H, 3.23. Found: C, 47.43; H, 2.97%.

2.6. Reaction of $Ru_3(CO)_7(\mu_3\text{-}COMe)[\mu\text{-}P(Ph)C{=}C(PPh_2)C(O)CH_2C(O)]$ (**4**) with PMe_3 to give $Ru_3(CO)_6(PMe_3)(\mu_3\text{-}COMe)[\mu\text{-}P(Ph)C{=}C(PPh_2)C(O)CH_2C(O)]$ (**7**) and $Ru_3(CO)_6(PMe_3)_2(\mu_2\text{-}COMe)[\mu\text{-}P(Ph)C{=}C(PPh_2)C(O)CH_2C(O)]$ (**8**)

0.17 g (0.18 mmol) of **4** and 30 mL CH_2Cl_2 were charged to a Schlenk tube and the contents cooled to −78 °C using an external dry ice/acetone bath. 0.50 mL of 0.47 M PMe_3 in THF (0.24 mmol) was next added and the vessel sealed to protect against the loss of the volatile PMe_3, with stirring continued with warming to room temperature. The initial red color of the solution slowly turned dark red as the reaction approached room temperature. Stirring was continued for an additional 4 h once room temperature had been reached and the solution examined by TLC. Compound **4** was completely consumed and two new spots corresponding to the PMe_3-substituted clusters **7** (R_f = 0.85) and **8** (R_f = 0.25) were observed by TLC using an eluent composed of 5:1 CH_2Cl_2/Et_2O. Both products were isolated by flash column chromatography using the same solvent system as employed in the TLC. Recrystallization of **7** from benzene/MeOH furnished **7** in 80% yield (0.14 g), while the combustion sample and X-ray quality crystals of **8** were obtained from a recrystallization using CH_2Cl_2/benzene. Yield of **8**: 26 mg (14% yield). The yield of **8** is greatly increased by using a threefold excess of PMe_3 relative to **4** or by treating **7** (isolated or in situ) with additional PMe_3. Compound **7**: Anal. Calc. for $C_{34}H_{29}O_9P_3Ru_3 \cdot 1/2C_6H_6$: C, 43.71; H, 3.17. Found: C, 44.17; H, 3.35%. Compound **8**: Anal. Calc. for $C_{37}H_{38}O_9P_4Ru_3 \cdot CH_2Cl_2$: C, 40.08; H, 3.54. Found: C, 40.29; H, 3.48%.

2.7. Photochemical conversion of $Ru_3(CO)_6(PMe_3)_2(\mu\text{-}COMe)[\mu\text{-}P(Ph)C{=}C(PPh_2)C(O)CH_2C(O)]$ (**8**) to **7** and $Ru_3(CO)_5(PMe_3)_2(\mu_3\text{-}COMe)[\mu\text{-}P(Ph)C{=}C(PPh_2)C(O)CH_2C(O)]$ (**9**)

A 0.15 g (0.14 mmol) sample of **8** was dissolved in ca. 25 mL of CH_2Cl_2 and irradiated between two GE Blacklight bulbs overnight.

Table 2
X-ray crystallographic data and processing parameters for **4**–**6**, **8**, and **9**

Compound	**4**	**5**	**6**	**8**	**9**
CCDC Entry No.	617376	617374	617375	617377	617378
Crystal system	Triclinic	Triclinc	Monoclinic	Triclinic	Monoclinic
Space group	$P\bar{1}$	$P\bar{1}$	$P2_1/n$	$P\bar{1}$	$P2_1/n$
a (Å)	10.8594(7)	9.857(1)	20.084(1)	12.1735(7)	11.929(1)
b (Å)	11.933(1)	10.5766(8)	12.7078(9)	13.1955(7)	13.399(1)
c (Å)	13.420(1)	17.594(2)	22.029(2)	15.6289(8)	28.775(2)
α (°)	86.983(8)	102.186(9)		113.616(4)	
β (°)	88.562(6)	105.19(1)	116.906(6)	93.533(5)	95.67(2)
γ (°)	75.961(8)	92.887(8)		89.956(5)	
V (Å^3)	1685.1(3)	1719.4(3)	5013.7(7)	2295.2(2)	4577(2)
Molecular formula	$C_{32}H_{20}O_{10}P_2Ru_3$	$C_{30}H_{20}O_9P_2Ru_3 \cdot 1/2C_7H_8$	$C_{49}H_{35}O_9P_3Ru_3 \cdot MeOH \cdot CH_2Cl_2$	$C_{37}H_{38}O_9P_4Ru_3 \cdot CH_2Cl_2$	$C_{36}H_{38}O_8P_4Ru_3 \cdot THF$
Fw	929.67	932.65	1280.93	1138.75	1097.91
Formula units per cell (Z)	2	2	4	2	4
$D_{calc.}$ (g/cm^3)	1.832	1.801	1.697	1.648	1.593
λ (Mo Kα), Å	0.71073	0.71073	0.71073	0.71073	0.71073
Absorption coefficient (cm^{-1})	14.49	14.19	11.33	12.58	11.44
R_{merge}	n/a	n/a	0.018	n/a	0.031
Abs. corr. factor	0.79/1.14	0.87/1.11	0.92/1.07	0.85/1.13	0.63/1.23
Total reflections	4166	4221	6470	5594	3474
Independent reflections	3746	2104	4657	4732	966
Data/res/parameters	3746/0/334	2104/0/263	4657/0/442	4732/0/506	966/0/225
R	0.0318	0.0467	0.0420	0.0315	0.0567
R_w	0.0347	0.0726	0.0444	0.0350	0.0661
GOF on F^2	1.82	0.95	1.09	1.10	0.91
Weights	$[0.04F^2 + (\sigma F)^2]^{-1}$	$[0.04F^2 + (\sigma F)^2]^{-1}$	$[0.04F^2 + (\sigma F)^2]^{-1}$	$[0.04F^2 + (\sigma F)^2]^{-1}$	$[0.04F^2 + (\sigma F)^2]^{-1}$
$\Delta\rho$(max), $\Delta\rho$(min) (e/Å^3)	0.74 near Ru(1)	0.88 near Ru(1), −0.24	0.92 near CH_2Cl_2	1.0 near CH_2Cl_2, −0.77	0.76 near THF

TLC examination of the solution the following day using CH_2Cl_2 as the eluent revealed the presence of **7** (major; $R_f = 0.25$) and a new spot (minor; $R_f = 0.15$), whose identity was later established as **9**. Both products were isolated by chromatographic separation, affording 86 mg of **7** (62%) and 15 mg (10%) of **9**. ESI-MS m/z: 1025.73 for [**9**+H]$^+$.

2.8. Kinetics studies on the conversion of *2* to *4*

The UV–Vis studies were carried out using a cluster concentration of ca. 10^{-4} M employing 1.0 cm quartz UV–Vis cells that were equipped with a high-vacuum Teflon stopcock to facilitate handling on the vacuum line. Solutions of **2** were prepared under argon and used immediately before each kinetic measurement. The Hewlett–Packard 8452A diode array spectrometer employed in our studies was configured with a variable-temperature cell holder and was connected to a VWR constant temperature circulator, allowing for the quoted temperatures to be maintained within ±0.5 K. The UV–Vis kinetics were monitored by following the decrease of the 420 nm absorbance band as a function of time for at least 4 half-lifes. The rate constants quoted in Table 4 were determined by non-linear regression analysis using the single exponential function [8]:

$$A(t) = A_\infty + \Delta A * e(-kt)$$

The activation parameters for the conversion of **2** to **4** were calculated from a plot of $\ln(k/T)$ versus T^{-1} [9], with the error limits representing the deviation of the data points about the least-squares line of the Eyring plot.

2.9. X-ray diffraction structures for *4*–*6*, *8*, and *9*

Single crystals of **4** suitable for X-ray crystallography were grown from a CH_2Cl_2 solution containing **4** that had been layered with hexane, with crystals of **5** · 1/2 toluene, grown from a toluene solution of **5** that had layered with hexane. The growth of X-ray quality crystals of **6** · CH_2Cl_2 · MeOH has already been described, while the crystals of **8** · CH_2Cl_2 and **9** · THF were grown from cluster solutions in CH_2Cl_2 and THF, respectively, that had been layered with hexane. In each case, a suitable crystal was chosen and sealed inside a Lindemann capillary tube, followed by mounting on an Enraf-Nonius CAD-4 diffractometer. After the cell constants were obtained, intensity data in the range of $2° \leqslant 2\theta \leqslant 44°$ were collected at 298 K and were corrected for Lorentz, polarization, and absorption (DIFABS). The structure for **4** was solved by SIR, and all non-hydrogen atoms were located with difference Fourier maps and full-matrix least-squares refinement. With the exception of the phenyl carbon atoms, all non-hydrogen atoms were refined anisotropically. The remaining four structures were all solved by using SHELX-86 and all non-hydrogen atoms were located with difference Fourier maps and full-matrix least-squares refinement. For **5** · 1/2C_7H_8, the three bridging were not located during refinement, and all of the non-hydrogens were refined anisotropically except for the carbon atoms. In the case of **6** · CH_2Cl_2 · MeOH, all of the non-hydrogen atoms except for the phenyl carbons were refined anisotropically, while all of the non-hydrogen atoms were refined anisotropically for **8** · CH_2Cl_2. All of the non-hydrogen atoms in **9** · THF had to be refined isotropically due to solvent loss and the poor quality of the crystal. The carbon-bound hydrogen atoms in all five cluster compounds were assigned to calculated positions and allowed to ride on the attached heavy atom. Table 2 summarizes the X-ray processing and data collection parameters, and Table 3 displays selected bond distances and angles for these clusters.

3. Discussion

3.1. Synthesis and spectroscopic data for *2* and *3*

The reaction between $HRu_3(CO)_{10}(\mu\text{-COMe})$ (**1**) and the diphosphine ligand bpcd proceeds readily in CH_2Cl_2 at room temperature in the presence of the oxidative-decarbonylation reagent Me_3NO (2 equiv.) [10]. TLC analysis of the reaction solution using a 1:1 mixture of CH_2Cl_2/hexane confirmed the near quantitative consumption of cluster **1** and bpcd and the presence of one major species ($R_f = 0.25$), whose identity was subsequently confirmed as $HRu_3(CO)_8(\mu\text{-COMe})$(bpcd) (**2**). The red-black material that remained at the origin of the TLC plate was also investigated by redeveloping the TLC plate using acetone as an eluent. The more polar solvent afforded a second spot that was ascribed to the phosphido-

Table 3
Selected bond distances (Å) and angles (degr) for **4**–**6**, **8**, and **9**[a]

Cluster **4**			
Bond distances			
Ru(1)–Ru(2)	2.8317(7)	Ru(1)–Ru(3)	2.7517(7)
Ru(2)–Ru(3)	2.8583(6)	Ru(1)–P(1)	2.334(2)
Ru(1)–P(2)	2.337(2)	Ru(1)–C(16)	2.126(7)
Ru(2)–P(2)	2.325(2)	Ru(2)–C(16)	2.179(6)
Ru(3)–C(11)	2.228(6)	Ru(3)–C(15)	2.230(6)
Ru(3)–C(16)	1.950(6)	C(11)–C(12)	1.489(8)
C(11)–C(15)	1.439(7)	C(12)–C(13)	1.529(8)
C(13)–C(14)	1.518(7)	C(14)–C(15)	1.464(8)
Bond angles			
P(1)–Ru(1)–P(2)	83.22(5)	P(1)–Ru(1)–C(16)	110.9(2)
P(2)–Ru(1)–C(16)	90.9(2)	P(2)–Ru(2)–C(16)	89.9(2)
C(11)–Ru(3)–C(15)	37.6(2)	C(16)–O(17)–C(18)	118.2(5)
Ru(3)–C(11)–P(1)	95.1(2)	Ru(3)–C(15)–P(2)	86.3(2)
Ru(3)–C(15)–C(11)	71.1(3)	Ru(1)–C(16)–Ru(2)	82.3(2)
Cluster **5**			
Bond distances			
Ru(1)–Ru(2)	2.926(3)	Ru(1)–Ru(3)	2.960(2)
Ru(2)–Ru(3)	2.972(2)	Ru(1)–P(1)	2.336(6)
Ru(1)–P(2)	2.304(6)	Ru(2)–P(2)	2.290(6)
Ru(2)–C(15)	2.06(2)	Ru(3)–P(2)	2.323(6)
C(11)–C(15)	1.39(3)	C(12)–C(13)	1.52(3)
C(13)–C(14)	1.51(3)	C(14)–C(15)	1.47(3)
Bond angles			
P(1)–Ru(1)–P(2)	90.8(2)	P(2)–Ru(2)–C(15)	96.3(6)
Ru(1)–P(1)–C(11)	110.6(7)	Ru(1)–P(2)–Ru(2)	79.1(2)
Ru(1)–P(2)–Ru(3)	79.5(2)	Ru(2)–P(2)–Ru(3)	80.2(2)
P(1)–C(11)–C(15)	125(1)	Ru(2)–C(15)–C(11)	127(1)
Cluster **6**			
Bond distances			
Ru(1)–Ru(2)	2.785(1)	Ru(1)–Ru(3)	2.8728(8)
Ru(2)–Ru(3)	2.8195(7)	Ru(1)–P(1)	2.308(2)
Ru(1)–P(2)	2.328(2)	Ru(1)–C(16)	2.215(8)
Ru(2)–C(11)	2.214(7)	Ru(2)–C(15)	2.246(8)
Ru(2)–C(16)	1.985(8)	Ru(3)–P(2)	2.340(2)
Ru(3)–P(3)	2.413(2)	Ru(3)–C(16)	2.097(7)
O(17)–C(16)	1.33(1)	O(17)–C(18)	1.434(9)
C(11)–C(12)	1.49(1)	C(11)–C(15)	1.445(9)
C(12)–C(13)	1.52(1)	C(13)–C(14)	1.503(9)
C(14)–C(15)	1.49(1)		
Bond angles			
P(1)–Ru(1)–P(2)	84.30(7)	P(1)–Ru(1)–C(1)	103.3(2)
P(1)–Ru(1)–C(2)	101.9(2)	P(1)–Ru(1)–C(16)	111.0(2)
P(2)–Ru(1)–C(1)	95.5(3)	P(2)–Ru(1)–C(2)	171.8(3)
P(2)–Ru(1)–C(16)	89.3(2)	C(3)–Ru(2)–C(11)	97.5(3)
C(3)–Ru(2)–C(15)	132.0(3)	C(11)–Ru(2)–C(15)	37.8(2)
C(11)–Ru(2)–C(16)	129.7(3)	C(15)–Ru(2)–C(16)	122.2(3)
P(2)–Ru(3)–P(3)	178.14(6)	P(2)–Ru(3)–C(16)	91.9(2)
P(3)–Ru(3)–C(16)	86.6(2)	C(5)–Ru(3)–C(16)	125.2(4)
C(6)–Ru(3)–C(16)	133.2(3)	Ru(2)–C(15)–P(2)	86.2(3)
Ru(1)–C(16)–Ru(2)	82.9(3)	Ru(1)–C(16)–Ru(3)	83.5(3)
Ru(2)–C(16)–Ru(3)	87.3(3)		
Cluster **8**			
Bond distances			
Ru(1)–Ru(2)	2.8610(6)	Ru(1)–C(11)	2.297(6)
Ru(1)–C(15)	2.177(5)	Ru(1)–C(16)	1.998(7)
Ru(2)–P(1)	2.411(2)	Ru(2)–P(2)	2.429(1)
Ru(3)–P(2)	2.455(1)	Ru(3)–P(3)	2.404(2)
Ru(3)–P(4)	2.357(2)	Ru(3)–O(14)	2.181(4)
Ru(3)–C(16)	2.098(6)	O(12)–C(12)	1.219(8)
O(14)–C(14)	1.285(7)	C(11)–C(12)	1.464(8)
C(11)–C(15)	1.467(8)	C(12)–C(13)	1.549(7)
C(13)–C(14)	1.526(9)	C(14)–C(15)	1.397(6)
Bond angles			
C(2)–Ru(1)–C(11)	123.0(3)	C(2)–Ru(1)–C(15)	155.5(2)
C(11)–Ru(1)–C(15)	38.2(2)	C(11)–Ru(1)–C(16)	128.5(2)
C(15)–Ru(1)–C(16)	90.3(2)	P(1)–Ru(2)–P(2)	84.35(5)
P(2)–Ru(3)–P(3)	98.19(5)	P(2)–Ru(3)–P(4)	160.98(7)
P(3)–Ru(3)–P(4)	95.09(6)	P(2)–Ru(3)–O(14)	85.13(9)
P(2)–Ru(3)–C(16)	78.2(2)	P(3)–Ru(3)–O(14)	92.1(1)
P(3)–Ru(3)–C(16)	175.6(1)	P(4)–Ru(3)–O(14)	80.8(1)

(*continued on next page*)

Table 3 (*continued*)

P(4)–Ru(3)–C(16)	89.0(1)	O(14)–Ru(3)–C(6)	176.3(2)
O(14)–Ru(3)–C(16)	90.0(2)	Ru(2)–P(2)–Ru(3)	125.31(6)
Ru(1)–C(16)–Ru(3)	117.7(3)		
Cluster **9**			
Bond distances			
Ru(1)–Ru(2)	2.855(5)	Ru(1)–Ru(3)	2.756(5)
Ru(2)–Ru(3)	2.814(6)	Ru(1)–P(1)	2.36(1)
Ru(1)–P(2)	2.37(1)	Ru(1)–C(16)	2.03(4)
Ru(2)–P(2)	2.37(1)	Ru(2)–P(3)	2.35(1)
Ru(2)–C(16)	2.07(4)	Ru(3)–P(4)	2.32(1)
Ru(3)–C(11)	2.24(1)	Ru(3)–C(15)	2.16(4)
Ru(3)–C(16)	2.02(4)	C(11)–C(12)	1.57(6)
C(11)–C(15)	1.47(6)	C(12)–C(13)	1.51(5)
C(13)–C(14)	1.44(6)	C(14)–C(15)	1.47(5)
Bond angles			
P(1)–Ru(1)–P(2)	79.9(4)	P(1)–Ru(1)–C(16)	115(1)
P(2)–Ru(1)–C(16)	91(1)	P(2)–Ru(2)–P(3)	93.1(4)
P(2)–Ru(2)–C(16)	89(1)	P(3)–Ru(2)–C(16)	153(1)
P(4)–Ru(3)–C(16)	91(1)	C(11)–Ru(3)–C(15)	39(1)
C(11)–Ru(3)–C(16)	127(2)	C(15)–Ru(3)–C(16)	117(1)
Ru(1)–P(2)–Ru(2)	74.2(4)	P(4)–Ru(3)–C(11)	103(1)
P(4)–Ru(3)–C(15)	141(1)	C(5)–Ru(3)–C(11)	110(2)
C(5)–Ru(3)–C(15)	101(2)	C(5)–Ru(3)–C(16)	122(2)

[a] Numbers in parentheses are estimated standard deviations in the least significant digits.

bridged cluster $HRu_3(CO)_8(Ph_2PH)[\mu\text{-}PPh_2C{=}CC(O)CH_2C(O)]$ (**3**). The products **2** and **3** were isolated by column chromatography and characterized by IR and NMR spectroscopies and combustion analyses. Compounds **2** and **3** are mildly air sensitive in solution, with those solutions exposed to oxygen exhibiting decomposition after several hours. The formulated structures for these clusters are shown below.

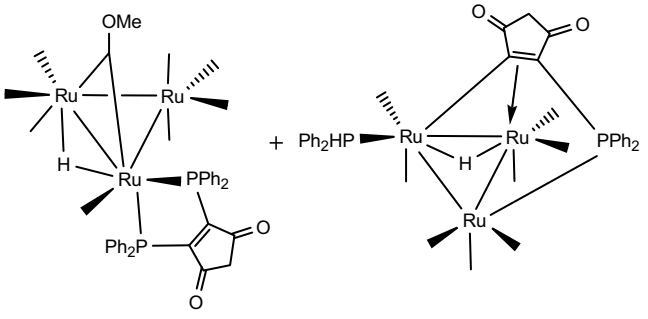

2 **3**

The IR spectrum of **2** shows terminal carbonyl bands at 2074 (s), 2037 (vs), 2000 (s), 1982 (s), 1974 (s), and 1946 (w, sh) cm^{-1}, in addition to two lower energy ν(CO) bands at 1746 and 1714 cm^{-1} associated with the vibrationally coupled symmetric and antisymmetric dione carbonyl groups belonging to the platform ring of the bpcd ligand [11]. The terminal ν(CO) bands for **2** are in excellent agreement with those data reported earlier by us for the related bma-substituted cluster $HRu_3(CO)_8(\mu\text{-}COMe)$(bma) [1]. The ^1H NMR spectrum exhibited characteristic resonances at δ −13.29, 3.41, and 4.07 that are readily assigned to the high-field hydride, methylene moiety of the bpcd ring, and bridging methoxy group. The overlapping aryl hydrogens were observed from δ 7.00–8.20. The chelation of the ancillary bpcd ligand in **2** was corroborated by the observation of two down-field ^{31}P singlets at δ 51.74 and 43.62 in the ^{31}P NMR spectrum. The presence of inequivalent ^{31}P resonances is consistent with the formulated structure for **2**, and is in keeping with those data reported in the triruthenium clusters $HRu_3(CO)_8(\mu\text{-}COMe)$(bma), $HRu_3(CO)_8(\mu_2\text{-}NCPh_2)$(bpcd), and $HRu_3(CO)_8(\mu_2\text{-}PPh_2)$(bpcd), where the diphosphine ligands are chelated to one of the hydride-bridged ruthenium centers [1,12,13].

The spectroscopic properties of **3** mirror those data reported by us for the diphenylphosphine-substituted cluster $HRu_3(CO)_8(Ph_2PH)[\mu\text{-}PPh_2C{=}CC(O)OC(O)]$, which was also isolated as a minor product from the reaction of **1** with bma. The loss of the bridging methylidyne moiety and the P–C bond activation of the bma ligand that accompany the formation of $HRu_3(CO)_8(Ph_2PH)[\mu\text{-}PPh_2C{=}CC(O)OC(O)]$ were unequivocally established by X-ray diffraction analysis [1]. Unlike $HRu_3(CO)_8(Ph_2PH)[\mu\text{-}PPh_2C{=}CC(O)OC(O)]$ which exists as a 9:1 mixture of stereoisomers in solution, **3** exhibits a single set of ^{31}P resonances at δ 7.70 and 32.28 for the coordinated Ph_2PH and Ph_2PC (dione ring) moieties, respectively.

The thermolysis of **1** with added bpcd was also investigated in 1,2-dichloroethane at ca. 80–90 °C as an alternative route to **2**. Heating an equimolar amount of **1** and bpcd does indeed afford **2**, as verified by TLC monitoring of the reaction solution, in addition to a new red cluster that was later shown to be $Ru_3(CO)_7(\mu_3\text{-}COMe)[\mu\text{-}P(Ph)C{=}C(PPh_2)C(O)CH_2C(O)]$ (**4**) (*vide infra*). Independent thermolysis reactions employing **2** were also performed and these reactions confirmed that the thermolysis of **2** does indeed produce **4**. These experiments indicate that the synthesis of **2** via the direct thermolysis of **1** with bpcd is not a viable synthetic route to **2** because the initially formed product is not stable and competitively transforms to **4**.

3.2. Synthesis, kinetics, and crystallographic data for *4*

Heating cluster **2** in either toluene or 1,2-dichloroethane leads to the rapid loss of CO and benzene and the formation of the phosphido-bridged cluster $Ru_3(CO)_7(\mu_3\text{-}COMe)[\mu\text{-}P(Ph)C{=}C(PPh_2)C(O)CH_2C(O)]$ (**4**). The formation of benzene was verified by GC–MS analysis. Compound **4** was observed as the predominant product, in addition to trace amounts of **1** (<1%), when preparative thermolysis reactions employing **2** were monitored by TLC. Compound **4** was readily isolated by column chromatography and characterized by NMR and IR spectroscopies and X-ray diffraction analysis. The thermolysis reaction of **2** to **4** is depicted in Eq. (2). Compound **4** displays terminal ν(CO) bands at 2075 (s), 2020 (vs), 1978 (m),

and 1968 (m) cm^{-1}, and the carbonyl bands belonging to dione moiety appear at 1708 (m) and 1682 (m) cm^{-1}. The shift to lower energy exhibited by these latter two ν(CO) bands relative to the dione ν(CO) bands in **2** indicates that the π bond of the cyclopenten-1,3-dione ring is coordinated to one of the ruthenium centers [14]. The ^{1}H NMR spectrum exhibits three sets of resonances at δ 7.20–7.84, 4.54, and 3.51 in a 15:3:2 integral ratio, respectively, whose assignments for three aryl rings, a bridging methylidyne moiety, and a bpcd-derived methylene group are consistent with the formulated structure for **4**. The two ^{31}P doublets recorded in the ^{31}P NMR spectrum at δ 83.15 and 37.15 are congruent with the presence of proximally situated phosphido and phosphine moieties, respectively, as found by us in other trimetallic clusters containing an activated bpcd ligand [13,15]. The ORTEP diagram of **4** is shown in Fig. 1, where the loss of one aryl ring is immediately verified. Compound **4** contains 48-valence electrons, and the triangular array of ruthenium atoms is face-capped by bridging methoxymethylidyne and P(Ph)C=CC(O)CH_2C(O)PPh_2 ligands, which serve as 3e- and 7e- donor ligands, respectively. The bond distances and angles associated with the latter ligand are in agreement with those values reported by us in related cluster systems containing the same ligand [13,15]. The seven ancillary CO groups are all linear and display bond distances and angles within acceptable limits.

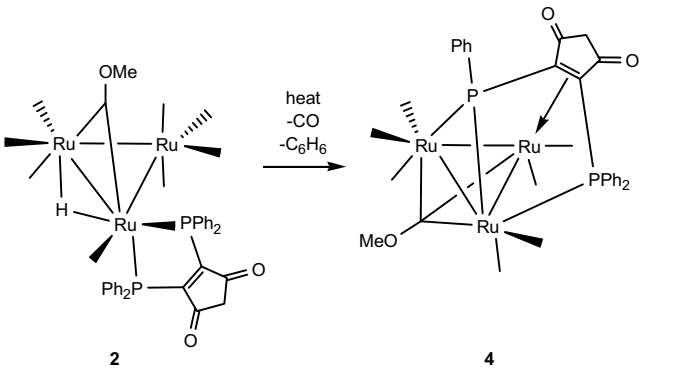

2 **4** (2)

The kinetics for the conversion of **2** to **4** were also investigated by UV–Vis spectroscopy over the temperature range of 320–343 K. Here the reaction rates were readily measured by following the decrease in the absorbance of the 420 nm band of **2**, with the rate constants presented in Table 4. The observed isosbestic points at 323, 400, and 464 nm confirm that the reaction is kinetically well-behaved and not subject to gross material loss. The nature of the solvent is not terribly important, as entries 2 and 3 in Table 4 exhibit nearly identical rate constants for reactions conducted in toluene and DCE. The effect of added CO on the reaction was also examined, and these data are seen in entries 5 and 6, where 1 atm of CO retards to the rate by a factor of ca. 10^2. On the basis of the first-order kinetics, CO inhibition, and the Eyring activation parameters [$\Delta H^{\ddagger}$ = 30.8(3) kcal/mol; $\Delta S^{\ddagger}$ = 19.6(8) eu], a mechanism involving a rate-limiting, unimolecular CO loss from **2** is supported [16]. The oxidative Ph–P bond cleavage experienced by the bpcd ligand and the elimination of benzene that accompany the formation of **4** must follow after the putative unsaturated species $HRu_3(CO)_7$(μ-COMe)(bpcd) has formed in the rate-limiting step of the reaction.

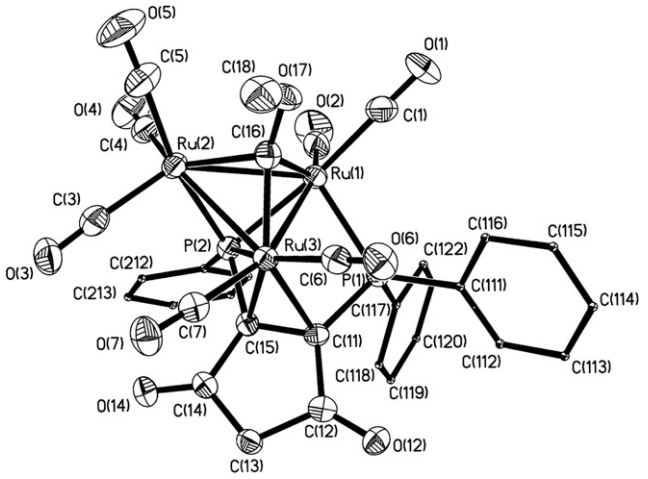

Fig. 1. ORTEP diagram of **4** showing the thermal ellipsoids at the 30% probability level.

3.3. Ligand substitution properties of *4*

The reactivity of **4** was next explored as part of our interest on the lability of the face-capping ligand P(Ph)C=CC(O)CH_2C(O)PPh_2 in associative ligand exchange processes where the π-bound alkene moiety serves as a coordinatively flexible ligand [17]. Scheme 1 illustrates the various reactions examined. Compound **4** reacts with H_2 (100 psi) at ca. 65 °C in toluene to furnish the phosphinidene-capped **5**. The ^{1}H NMR spectrum of **5** exhibits three distinct hydride resonances at δ −17.41, −18.25, and −18.70 in agreement with a structure containing three hydride-bridged Ru–Ru bonds. The 15 aromatic hydrogens belonging to the three phenyl groups appear as a set of overlapping resonances from δ 7.05–7.80 while the methylene hydrogens of the carbocyclic dione ring appear as a singlet at δ 2.95. The two ^{31}P resonances recorded at δ 259.32 and 18.17 may be confidently assigned to the face-capping phosphinidene and phosphine ligands, respectively. The molecular structure of **5**, which is depicted in Fig. 2, confirms the loss of the methoxymethylidyne ligand and the cleavage of the PhP–C(dione) bond belonging to the face-capping P(Ph)C=CC(O)CH_2-C(O)PPh_2 ligand in **4**. Activation of the latter ligand leads to the observed μ_3-PPh phosphinidene moiety and the edge-bridging C=CC(O)CH_2C(O)PPh_2 ligand in **5**. Compound **5** is electron precise with 48-valence electrons and displays an average Ru–Ru bond distance of 2.953 Å, whose value is consistent with Ru–Ru bond distances found in other polynuclear ruthenium clusters [18]. Each Ru–Ru vector contains an edge-bridged hydride that lies below the metallic plane capped by the μ_3-PPh group similar to those pseudo-axial hydride ligands in the triruthenium clusters $H_2Ru_3(CO)_8$($PMePh_2$)(μ_3-PPh) and $H_2Ru_3(CO)_9$(μ_3-PPh) [19]. The 3e- ligand C=CC(O)CH_2C(O)PPh_2 spans the Ru(1)–Ru(2) vector in a plane roughly parallel to the triangular array of ruthenium atoms and exhibits a Ru(2)–C(15) σ bond of 2.06(2) Å and a Ru(1)–P(1) dative bond of 2.336(6) Å, whose distances are similar to those distances

Table 4
Experimental rate constants for the conversion of **2** to **4**[a]

Entry No.	Temperature (K)	Solvent	$10^4 k$ (s^{-1})
1	320.2	Toluene	1.28 ± 0.01
2	320.2	Toluene	1.36 ± 0.01[b]
3	320.2	DCE	1.31 ± 0.02
4	326.5	Toluene	3.68 ± 0.12
5	333.3	Toluene	8.68 ± 0.04
6	333.3	Toluene	0.10 ± 0.01[c]
7	338.2	Toluene	17.3 ± 0.3
8	343.1	Toluene	31.7 ± 0.2

[a] The UV–Vis kinetic data were collected in the specified solvent using 2.2×10^{-4} M solution of cluster **2** by following the decrease in the absorbance of the 420 nm band.
[b] Reaction carried out with a 1.1×10^{-4} M solution of cluster **2**.
[c] Reaction carried out under 1 atm of CO.

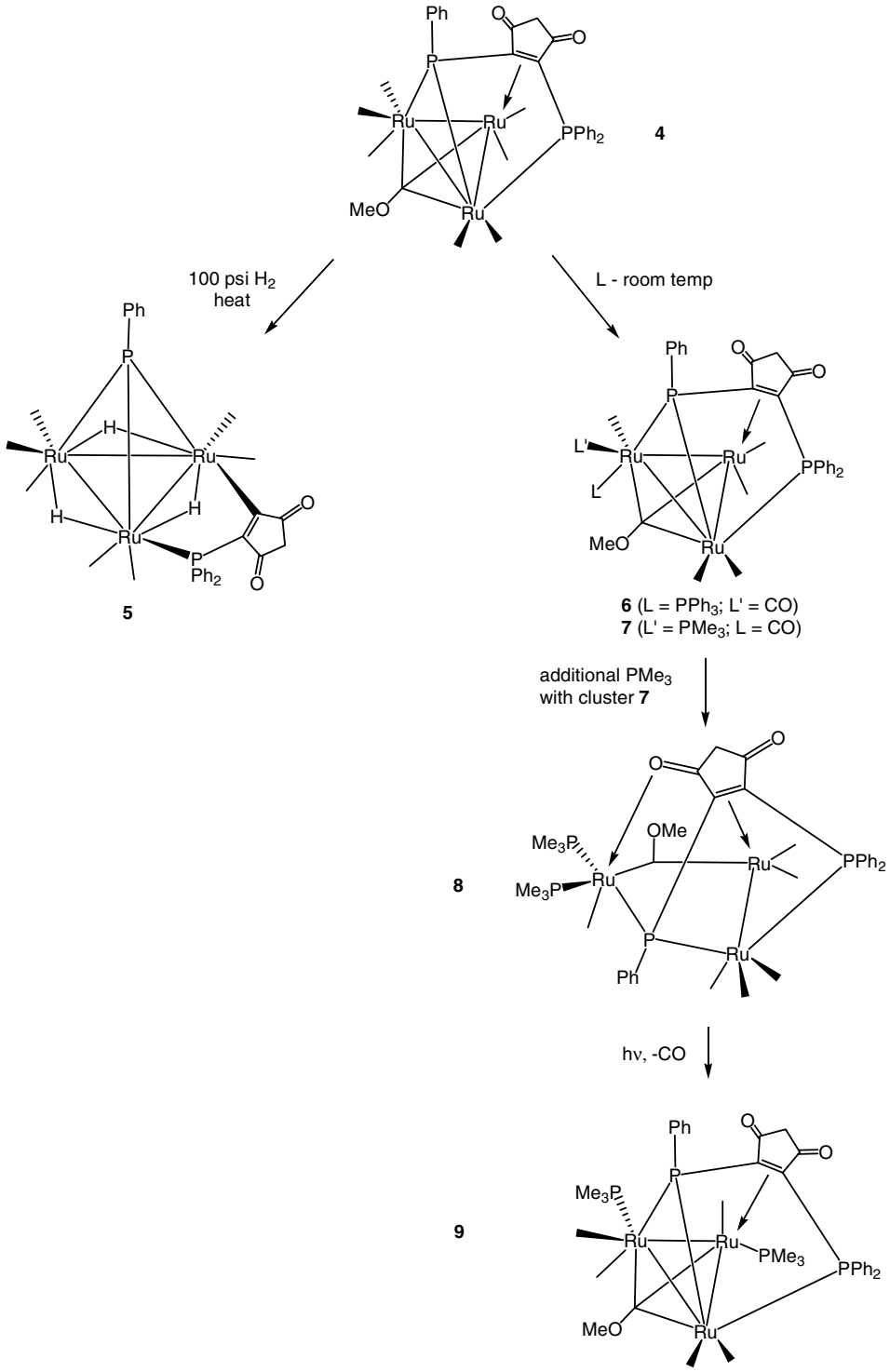

Scheme 1.

reported by us in the cluster compound $Ru_3(CO)_7[\mu\text{-}C{=}CC(O)CH_2\text{-}C(O)PPh_2](\mu\text{-}PPh_2)(\mu_3\text{-}NPh)$ [20].

Thermolysis of **4** with PPh_3 (1 equiv.) in CH_2Cl_2 gave the mono-substituted cluster **6** in high yield. The ^{31}P NMR spectrum of **6** in $CDCl_3$ at room temperature revealed the presence of a single isomer based on one set of resonances at δ 85.01 (dd), 42.21 (d), and 41.08 (d), where the former resonance is readily assigned to the phosphido moiety. The phosphido resonance appears as a doublet-of-doublets with disparate splittings of 156 Hz and 7 Hz,. The small 7 Hz splitting derives from geminal coupling between the two phosphorus atoms in the face-capping $P(Ph)C{=}CC(O)CH_2\text{-}C(O)PPh_2$ ligand, and the larger coupling of 156 Hz indicates that the PPh_3 must be oriented *trans* to the phosphido moiety [21]. The ^1H NMR spectrum shows an aromatic multiplet from δ 7.10–7.90 that integrates for 30H, supporting the addition of one PPh_3 ligand to **6**, in addition to an AB quartet for the diastereotopic methylene hydrogens that is centered at δ 3.45, and a three proton singlet at δ 3.02 for the methoxymethylidyne moiety. The exact lo-

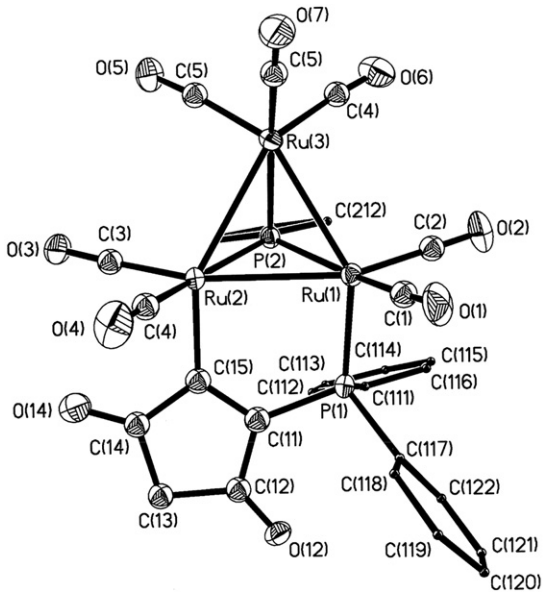

Fig. 2. ORTEP diagram of **5** · $1/2C_7H_8$ showing the thermal ellipsoids at the 30% probability level. The solvent molecule has been omitted for clarity.

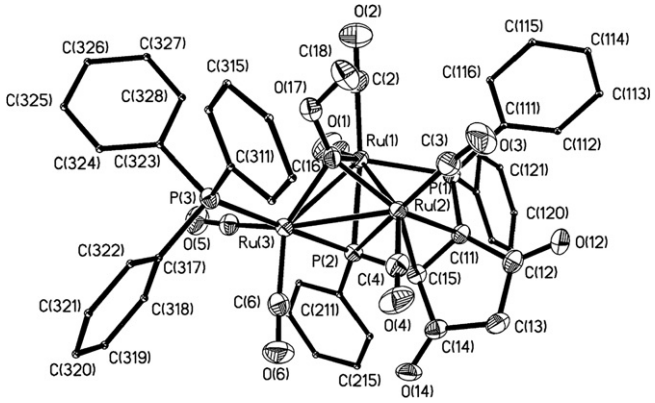

Fig. 3. ORTEP diagram of **6** · CH_2Cl_2 · MeOH showing the thermal ellipsoids at the 30% probability level. The solvents molecule have been omitted for clarity.

cus of the PPh_3 ligand in **6** was established by X-ray crystallography. The molecular structure of **6**, as the CH_2Cl_2 and MeOH solvates, shown in Fig. 3 confirms the formal substitution of CO by PPh_3 in this reaction. The basic polyhedral architecture in **6** resembles that of **4**, insomuch that the triangular array of ruthenium atoms is capped by the 3e- COMe and 7e- P(Ph)C═CC(O)CH_2-C(O)PPh_2 donor ligands. The Ru–Ru bond distances range from 2.785(1) Å [Ru(1)–Ru(2)] to 2.8728(8) Å [Ru(1)–Ru(3)], and exhibit a mean distance of 2.826 Å. The PPh_3 ligand is attached to Ru(3) and is situated *cis* to the μ_3-COMe ligand and *trans* to phosphido atom P(2). The bond angles of 86.6(2)° for the P(3)–Ru(3)–C(16) atoms and 178.14(6)° for P(2)–Ru(3)–P(3) atoms are in concert with the stereochemical assignments of the PPh_3 relative to the face-capping ligands. The remaining bond distances and angles exhibit values typical for such groups and require no comment.

Treatment of **4** in CH_2Cl_2 at −78 °C with a slight excess of PMe_3, followed by warming to room temperature, leads to the formation of two new products, as verified by TLC analysis. The new clusters were isolated by chromatographic separation over silica gel and characterized in solution by IR and NMR spectroscopies. The faster moving product, cluster **7**, exhibited spectral data consistent with the substitution of a CO group by a PMe_3 ligand. Compound **7** displays terminal ν(CO) bands at 2032 (m), 2002 (vs), 1968 (m), and 1994 (sh) cm^{-1}, and these IR data qualitatively mimic the IR spectral data from the PPh_3-substituted cluster **6**. The electron rich PMe_3 ligand in **7** does not appear to promote a significant shift of the terminal ν(CO) bands to lower frequencies relative to **6**, a trend commonly found in other clusters containing different PR_3 ligands [22]. The increased electron density in **7** vis-á-vis **6** is clearly manifested in the IR frequencies of the vibrationally coupled symmetric and antisymmetric ν(CO) bands of the dione ring. These ν(CO) bands in **7** appear at 1693 and 1670 cm^{-1}, and are 14 cm^{-1} and 11 cm^{-1}, respectively, lower in energy than the identical dione carbonyl stretching bands in **6**. That the ancillary P(Ph)C═CC(O)CH_2C(O)PPh_2 ligand serves as a suitable repository for excess electron density is supported by electrochemical experiments and MO calculations on related compounds bearing a bpcd ligand, where an accessible low-lying π^* orbital on the dione ring has been shown to function as an energetically accessible electron reservoir [23]. The three ^{31}P NMR resonances observed at δ 80.95, 39.22, and −10.40, all of which appear as doublets-of-doublets, are assigned to the μ-phosphido, PPh_2(dione), and PMe_3 ligands, respectively. The magnitudes of the phosphorus–phosphorus coupling constants provide important insight into the stereochemical disposition of the ancillary PMe_3 ligand relative to the cluster polyhedron. The similarity in the IR spectra of **6** and **7** argues for products that have a common phosphine regiochemistry, and this places the PMe_3 ligand in **7** at the same ruthenium atom as found in **6**. Whereas the ^{31}P NMR and X-ray diffraction data establish the *trans* relationship between the PPh_3 ligand and the bridging phosphido moiety in **6**, the J_{P-P} values of 19 Hz and 15 Hz exhibited by the phosphido group in **7** mandate a basal PMe_3 ligand. Scheme 1 shows the PMe_3 ligand at one of the two possible basal sites, either of which would yield a structure that is consistent with the spectroscopic data.

The minor product, cluster **8**, isolated from the reaction between **4** and PMe_3 displayed NMR spectral and combustion data supporting the formation of a triruthenium cluster containing two PMe_3 ligands. The origin of **8** was subsequently established through the independent reaction of **7** with a slight excess of PMe_3, giving **8** in near quantitative yield. The IR spectrum of **8** presented an interesting conundrum since only one ν(CO) band was observed for the dione moiety, and the four ^{31}P resonances recorded at δ 27.93, 2.12, −12.27, and −52.15 did little to help establish the identity of **8**. Accordingly, cluster **8** was subjected to X-ray crystallographic analysis, with Fig. 4 showing the molecular structure of **8**, as the CH_2Cl_2 solvate. Immediately obvious is the gross polyhedral alteration experienced by **8** relative to the metallic motif displayed by clusters **4** and **6**. Compound **8** contains 52-valence electrons, and this number is four electrons in excess of the electron-precise count of 48e- associated with triangular clusters. The cleavage of two of the three original Ru–Ru bonds that defined the triangular array of metal atoms in **7** is understood within the context of polyhedral skeletal electron pair (PSEP) theory [24]. The extra 4e- in **8** can be traced to the coordination of a second PMe_3 ligand and one of the dione's carbonyl groups to the Ru(3) atom. This latter Ru(3) center is formally six-coordinate and may be viewed as possessing a distorted octahedral geometry. The Ru(1)–Ru(2) vector exhibits a bond distance of 2.8610(6) Å in agreement with its single-bond designation [25], while the internuclear distances in excess of 3.50 Å for the Ru(1)···Ru(3) atoms and 4.30 Å for the Ru(2)···Ru(3) atoms clearly preclude any direct bonding interactions between these ruthenium centers. The P(Ph)C═CC(O)CH_2C(O)PPh_2 ligand in **8** functions as a 9e- donor and binds all three metals via the phosphido moiety (3e-), tertiary phosphine ligand (2e-), alkene π bond (2e-), and one dione carbonyl group (2e-). The O(14)–Ru(3) vector that defines the dative bond formed between the dione C(14)O(14) carbonyl group and the Ru(3) atom reveals a bond distance of 2.181(4) Å, whose value closely matches those distances in the other ruthenium cluster compounds containing an oxygen-coordinated carbonyl li-

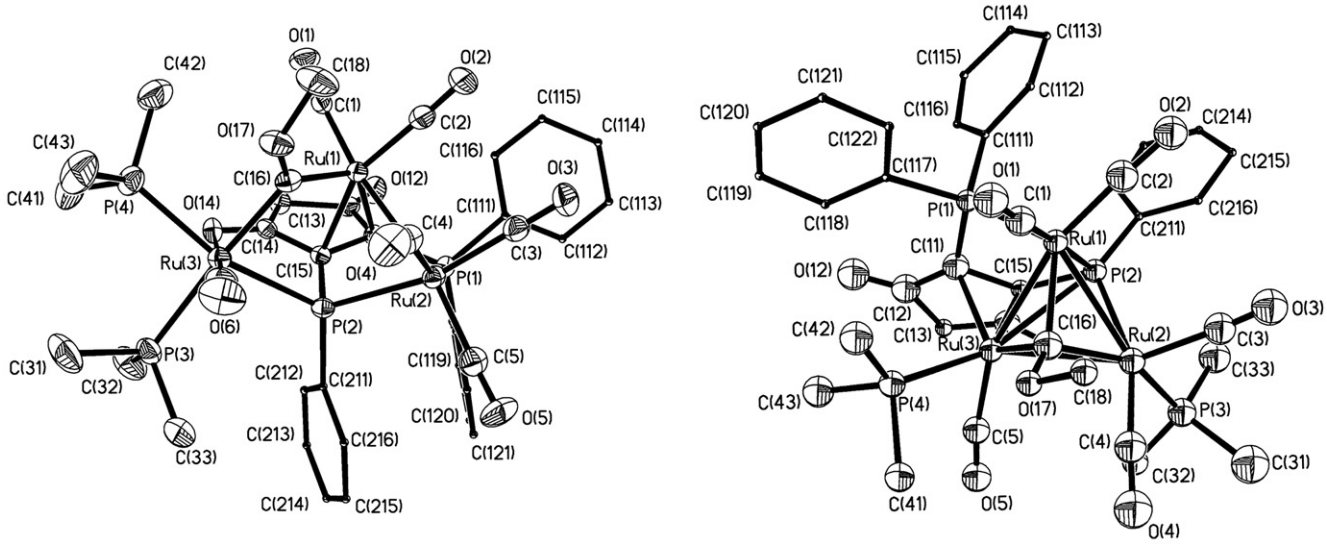

Fig. 4. ORTEP diagrams of **8** · CH_2Cl_2 (left) and **9** · THF (right) showing the thermal ellipsoids at the 30% probability level. All solvent molecules have been omitted for clarity.

gand [26]. While the bond distances for the Ru(1)–C(16) [1.998(7) Å] and Ru(3)–C(16) [2.098(6) Å] vectors associated with the bridging methoxymethylidyne moiety are comparable to those distances in the parent cluster $HRu_3(CO)_{10}(\mu\text{-COMe})$ and other polynuclear ruthenium compounds that contain this ligand [27,28], the bond angle subtended by the Ru(1)–C(16)–Ru(3) atoms [117.7(3)°] is understandably larger by ca. 28° as compared to the related angle(s) in edge-bridged μ-COMe and face-bridged μ_3-COMe complexes [27,28].

The observed structure of **8** facilitates the unequivocal assignment of the four ^{31}P resonances recorded in the NMR spectrum. The large $^2J_{P-P}$ value of 244 Hz is attributed to coupling between the P(2) and P(4) atoms, based on the nearly linear bond angle of 160.98(7)° found for the P(2)–Ru(3)–P(4) linkage. The assignment of the high-field ^{31}P resonance at δ −52.15 to the phosphido moiety P(2) is supported by the structural data and is congruent with the established trend exhibited by such ligands and their ligation of non-bonding metal centers [29]. The bond angles for the P(1)–Ru(2)–P(2) [84.35(5)°], P(2)–Ru(3)–P(3) [98.19(5)°], and P(3)–Ru(3)–P(4) [95.09(6)°] linkages confirm the near orthogonal relationship that exists between these phosphorus centers, leading to smaller $^2J_{P-P}$ values between these phosphorus centers. Chemical shifts arguments and ^{31}P data from other cluster analogues facilitate the ^{31}P assignments in **8**, as depicted below.

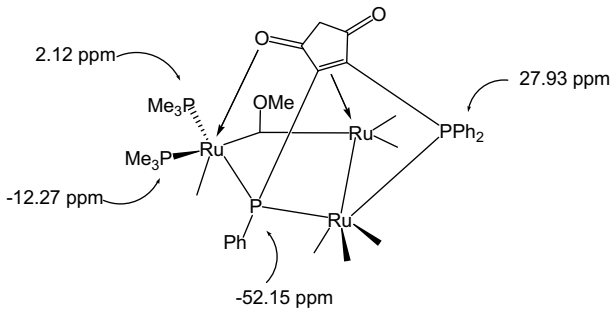

Compound **8** is photosensitive in solution, and irradiation of **8** with 366 nm light yields clusters **7** (major) and **9** (minor) as the principal products. The ESI mass spectrum of **9** gave a pseudomolecular ion at *m*/*z*: 1025.73 for $[\mathbf{9}+H]^+$ that supported the loss of only one CO ligand from **8**, and the ^{31}P NMR spectrum revealed four resonances at δ −9.45, 7.80, 48.50, and 73.72, fully consistent with the formulated structure of **9** that is depicted in Scheme 1. The two highest field resonances represent the PMe_3 ligands, with the remaining resonances attributed to the face-capping $P(Ph)C{=}CC(O)CH_2C(O)PPh_2$ ligand. The ORTEP diagram of **9**, as the THF solvate, is shown in Fig. 4, where the formal loss of one CO group, conversion of the bridging $P(Ph)C{=}CC(O)CH_2C(O)PPh_2$ ligand from a 9e- to a 7e- donor, and ring closure of the metallic polyhedron are confirmed. Compound **9** contains 48-valence electrons and is electron precise. The Ru–Ru bond distances range from 2.756(5) Å [Ru(1)–Ru(3)] to 2.855(5) Å [Ru(1)–Ru(2)], revealing the presence of an asymmetric metallic core in **9**. The vicinal PMe_3 ligands are attached to the Ru(2) and Ru(3) atoms and exhibit a P(3)–Ru(2)–Ru(3)–P(4) dihedral angle of ca. 127°. The bond angles for the P(4)–Ru(3)–C(16) [91(1)°] and P(3)–Ru(2)–C(16) [153(1)°] linkages indicate that the ancillary PMe_3 ligands are situated syn and anti, respectively, to the face-capping methoxymethylidyne moiety. The five terminal Ru–CO ligands display bond distances and angles fall within acceptable ranges for such groups, with the remaining bond distances and angles unremarkable relative to the other clusters presented here.

4. Conclusions

CO substitution in cluster $HRu_3(CO)_{10}(\mu\text{-COMe})$ by the diphosphine ligand bpcd gives the bpcd-chelated cluster $HRu_3(CO)_8(bpcd)(\mu\text{-COMe})$ (**2**) as the principal reaction product. Facile loss of benzene occurs on mild heating to afford the reactive cluster $Ru_3(CO)_7(\mu_3\text{-COMe})[\mu\text{-}P(Ph)C{=}C(PPh_2)C(O)CH_2C(O)]$ (**4**), whose chemistry with H_2 and phosphine ligands has been investigated. The face-capping $P(Ph)C{=}C(PPh_2)C(O)CH_2C(O)$ has been shown to function as either a 7e- or 9e- donor ligand, in addition to facilitating the expansion of the Ru_3 polyhedron in the reaction of **7** → **8**. Future studies will explore the catalytic properties of these and other cluster compounds that contain a coordinative flexible face-capping $P(Ph)C{=}C(PPh_2)C(O)CH_2C(O)$ ligand.

5. Supplementary material

CCDC 617376, 617374, 617375, 617377 and 617378 contain the supplementary crystallographic data for **4**, **5**, **7**, **8** and **9**. These data can be obtained free of charge from The Cambridge Crystallographic Data Centre via www.ccdc.cam.ac.uk/data_request/cif.

Acknowledgements

We thank Prof. Guido F. Verbeck for the use of his mass spectrometer and Ms. Nicole Ledbetter for recording the ESI-MS of cluster **9**. Financial support from the Robert A. Welch Foundation (Grant B-1093-MGR) is greatly appreciated.

References

[1] S.G. Bott, H. Shen, S. Kandala, N.H. Phan, M.G. Richmond, J. Coord. Chem. 60 (2007) 1223.
[2] (a) For reports on the silica gel promoted hydrolysis of the anhydride moiety of the bma ligand in related polynuclear compounds, see: K. Yang, S.G. Bott, M.G. Richmond, Organometallics 14 (1995) 2387;
(b) S.G. Bott, K. Yang, M.G. Richmond, J. Organomet. Chem. 689 (2005) 791.
[3] (a) K. Yang, J.M. Smith, S.G. Bott, M.G. Richmond, Organometallics 12 (1993) 4779;
(b) K. Yang, S.G. Bott, M.G. Richmond, Organometallics 13 (1994) 3788;
K. Yang, S.G. Bott, M.G. Richmond, Organometallics 14 (1995) 4977;
(c) K. Yang, J.A. Martin, S.G. Bott, M.G. Richmond, Organometallics 15 (1996) 2227;
(d) S.G. Bott, K. Yang, M.G. Richmond, J. Organomet. Chem. 690 (2005) 3067;
(e) W.H. Watson, B. Poola, M.G. Richmond, J. Organomet. Chem. 691 (2006) 5579.
[4] M.I. Bruce, C.M. Jensen, N.L. Jones, Inorg. Synth. 26 (1989) 259.
[5] J.B. Keister, J.R. Shapley, D.A. Strickland, Inorg. Synth. 27 (1990) 196.
[6] (a) D.T. Mowry, J. Am. Chem. Soc. 72 (1950) 2535;
(b) D. Fenske, H.J. Becher, Chem. Ber. 107 (1974) 117;
(c) D. Fenske, H.J. Becher, Chem. Ber. 108 (1975) 2115.
[7] D.F. Shriver, The Manipulation of Air-Sensitive Compounds, McGraw-Hill, New York, 1969.
[8] The rate calculations were performed by using the commercially available program ORIGIN6.0. Here the initial (A_0) and final (A_∞) absorbances and the rate constant (k) were floated to give the quoted least-squares value for first-order rate constant k.
[9] B.K. Carpenter, Determination of Organic Reaction Mechanisms, Wiley Interscience, New York, 1984.
[10] (a) U. Koelle, J. Organomet. Chem. 133 (1977) 53;
(b) M.O. Albers, N.J. Coville, Coord. Chem. Rev. 53 (1984) 227.
[11] C.N.R. Rao, Chemical Applications of Infrared Spectroscopy, Academic Press, New York, 1963.
[12] W.H. Watson, M.A. Mandez-Rojas, Y. Zhao, M.G. Richmond, J. Chem. Crystallogr. 33 (2003) 767.
[13] S.G. Bott, H. Shen, M.G. Richmond, J. Organomet. Chem. 690 (2005) 3838.
[14] (a) H. Shen, S.G. Bott, M.G. Richmond, Organometallics 14 (1995) 4625;
(b) S.G. Bott, K. Yang, J.C. Wang, M.G. Richmond, Inorg. Chem. 39 (2000) 6051;
(c) S.G. Bott, K. Yang, M.G. Richmond, J. Organomet. Chem. 689 (2004) 791.
[15] (a) S.G. Bott, H. Shen, R.A. Senter, M.G. Richmond, Organometallics 22 (2003) 1953;
(b) W.H. Watson, S.G. Bodige, K. Ejsmont, J. Liu, M.G. Richmond, J. Organomet. Chem. 691 (2006) 3609.
[16] (a) D.J. Darensbourg, Adv. Organomet. Chem. 21 (1982) 113;
(b) M.G. Richmond, J.K. Kochi, Inorg. Chem. 25 (1986) 1334.
[17] (a) K. Yang, S.G. Bott, M.G. Richmond, Organometallics 14 (1995) 919. 2718;
(b) C.G. Xia, K. Yang, S.G. Bott, M.G. Richmond, Organometallics 15 (1996) 4480.
[18] (a) A.J. Deeming, S. Doherty, N.I. Powell, Inorg. Chim. Acta 198–200 (1992) 469;
(b) P. Frediani, C. Faggi, S. Papaleo, A. Salvini, M. Bianchi, F. Piacenti, S. Ianelli, M. Nardelli, J. Organomet. Chem. 536–537 (1997) 123;
(c) A.J. Deeming, C.S. Forth, M.I. Hyder, S.E. Kabir, E. Nordlander, F. Rodgers, B. Ullmann, Eur. J. Inorg. Chem. (2005) 4352.
[19] (a) M.I. Bruce, E. Horn, O.B. Shawkataly, M.R. Snow, E.R.T. Tiekink, W.L. Williams, J. Organomet. Chem. 316 (1986) 187;
(b) F. Iwasaki, M.J. Mays, P.R. Raithby, P.L. Taylor, P.J. Wheatley, J. Organomet. Chem. 213 (1981) 185.
[20] S.G. Bott, H. Shen, M.G. Richmond, J. Organomet. Chem. 689 (2004) 3426.
[21] (a) P.E. Garrou, Chem. Rev. 81 (1981) 229;
(b) A.J. Carty, S.A. MacLaughlin, D. Nucciarone, in: J.G. Verkade, L.D. Quin (Eds.), Phosphorus-31 NMR Spectroscopy in Stereochemical Analysis: Organic Compounds and Metal Complexes, VCH Publishers, New York, 1987 (Chapter 16).
[22] (a) C.A. Tolman, Chem. Rev. 77 (1977) 313;
(b) D. Sonnenberger, J.D. Atwood, Inorg. Chem. 20 (1981) 3243;
(c) D.J. Darensbourg, B.S. Peterson, R.E. Schmidt Jr., Organometallics 1 (1982) 306.
[23] (a) H.J. Becher, D. Fenske, M. Heyman, Z. Anorg. Allg. Chem. 475 (1981) 27;
(b) D.R. Tyler, Acc. Chem. Res. 24 (1991) 325;
(c) D.M. Schut, K.J. Keana, D.R. Tyler, P.H. Rieger, J. Am. Chem. Soc. 117 (1995) 8939;
(d) R. Meyer, D.M. Schut, K.J. Keana, D.R. Tyler, Inorg. Chim. Acta 240 (1995) 405;
(e) N.W. Duffy, R.R. Nelson, M.G. Richmond, A.L. Rieger, P.H. Rieger, B.H. Robinson, D.R. Tyler, J.C. Wang, K. Yang, Inorg. Chem. 37 (1998) 4849.
[24] D.M.P. Mingos, D.J. Wales, Introduction to Cluster Chemistry, Prentice Hall, Englewood Cliffs, NJ, 1990.
[25] A.G. Orpen, L. Bramer, F.H. Allen, O. Kennard, D.G. Watson, R. Taylor, J. Chem. Soc., Dalton Trans. (1989) S1.
[26] (a) C.J. Adams, M.I. Bruce, B.W. Skelton, A.H. White, J. Cluster Sci. 5 (1994) 419;
(b) C.S.-W. Lau, W.-T. Wong, J. Chem. Soc., Dalton Trans. (1998) 391;
(c) C.J. Adams, M.I. Bruce, M.J. Liddell, B.W. Skelton, A.H. White, Organometallics 11 (1992) 1182;
(d) D. Heineke, H. Vahrenkamp, J. Organomet. Chem. 451 (1993) 147.
[27] M.R. Churchill, L.R. Beanan, H.J. Wasserman, C. Bueno, Z.A. Rahman, J.B. Keister, Orgaometallics 2 (1983) 1179.
[28] (a) L.W. Bateman, M. Green, K.A. Mead, R.M. Mills, I.D. Salter, F.G.A. Stone, P. Woodward, J. Chem. Soc., Dalton Trans. (1983) 2599;
(b) Y. Chi, S.-H. Chuang, B.-F. Chen, S.-M. Peng, G.-H. Lee, J. Chem. Soc., Dalton Trans. (1990) 3033;
(c) K.A. Johnson, W.L. Gladfelter, Organometallics 9 (1990) 2101;
(d) J. Evans, P.M. Stroud, M. Webster, Acta Crysallogr., Sect. C 46 (1990) 2334.
[29] (a) A.J. Carty, Adv. Chem. Ser. 196 (1982) 1963;
(b) W.C. Mercer, R.R. Whittle, E.W. Burkhardt, G.L. Geoffroy, Organometallics 4 (1985) 68.